



# Modelling of Memory Effects in Devices and Circuits with an Emphasis on Power Amplifiers

Dr Steve Maas & Andy Wallace  
Applied Wave Research Ltd (Europe)

Email: [awallace@awrcorp.com](mailto:awallace@awrcorp.com)  
2 Huntinggate, Hitchin, Herts, UK. SG4 0TJ

## Abstract

*In this presentation we discuss memory-effects of various classes and how these can be modelled using a system simulator. The methodology is based on using Volterra kernels from a number of harmonic balance simulations or measurements of the circuit under consideration and transforming the kernels into discrete time-domain convolutions. The time-domain representation of the kernels enables a straightforward implementation in complex-envelope system simulator. Once the Volterra model has been constructed, the full power of the system simulator can be exploited to simulate the device under test using complex signals used to capture the statistics of arbitrary wide-band excitation, e.g. WCDMA signal readily available in the simulator.*

## Introduction

The design of behavioural models that incorporate both static and dynamic nonlinearities is, at present, a dominant topic in nonlinear circuit and system research. Many methods have been proposed. Some are based on established methods for nonlinear system analysis such as Volterra series, Wiener functionals, polyspectral models, as well as AM-AM/AM-PM (Hammerstein) approaches. Others are purely *ad hoc*, with validity established only by limited experimental testing. The research community has consistently shown a preference for established methods over newer ideas, whatever their purported benefits. Indeed, the capabilities and limitations of established methods are better understood than those of *ad hoc* ones, so models based on such methods are not likely to be used inappropriately. In contrast, the uncertainty of the limitations of newer approaches could leave the user with a nasty surprise.

It appears that the research community is converging on Volterra methods as the primary tool for nonlinear behavioural modelling. Volterra methods can accommodate dynamic nonlinearities and memory effects, as well as static nonlinearities, in a very natural way [1-4]. The model proposed here is essentially a classical Volterra approach. Its novelty lies less in the model than in the use of a special method, which has been validated theoretically, for determining the time-domain kernels. Much of this work was performed in 2003 by Prof. J. C. Pedro of the University of Aveiro, while on sabbatical at AWR. The work, and the model, are described in his report [5]. The model is similar in many ways to an approach proposed earlier [6].

A well known limitation of Volterra analysis is its restriction to weak nonlinearities. For system analysis, this restriction is not as severe as it may seem, as most types of transmitter or receiver components are pseudo linear and thus can be modelled acceptably by Volterra methods. This includes such components as class-AB cellular power amplifiers, which are ideally linear, in terms of first-zone input and output, although a class-AB amplifier circuit itself is strongly nonlinear. Although amplifiers having strongly nonlinear transfer characteristics, such as GSM cellular power amplifiers, cannot be modelled in this manner, the kinds of results provided by a Volterra model, such as ACPR sidebands, are not relevant for them. In any case, strongly nonlinear amplifiers can be modelled acceptably in other ways.



## VSS Model

The model is essentially a classical implementation of what might be called a *finite impulse response* (FIR) Volterra “filter.” In this case, the output,  $w(t)$ , of the modelled two-port having excitation  $s(t)$  is given, in general, by:

$$\begin{aligned}
 w(t) = & \int_{-\infty}^{\infty} h_1(\tau) s(t - \tau) d\tau \\
 & + \int_{-\infty}^{\infty} \int_{-\infty}^{\infty} h_2(\tau_1, \tau_2) s(t - \tau_1) s(t - \tau_2) d\tau_1 d\tau_2 \\
 & + \int_{-\infty}^{\infty} \int_{-\infty}^{\infty} \int_{-\infty}^{\infty} h_3(\tau_1, \tau_2, \tau_3) s(t - \tau_1) s(t - \tau_2) s(t - \tau_3) d\tau_1 d\tau_2 d\tau_3 + \dots
 \end{aligned} \tag{1}$$

where  $h_1(\tau)$  is the linear impulse response of the system and  $h_n(\tau_1, \tau_2, \dots, \tau_n)$  is the  $n$ th-order Volterra kernel of the system. For a narrowband signal, where we are concerned only with the “first-zone” response (i.e., limited frequency components near the centre frequency  $\omega_0$ ), we need only the linear and odd-order terms. To keep the identification problem under control, we limit ourselves to third order. Converting the continuous-time expression to discrete time gives the well known expression:

$$\begin{aligned}
 w(t) = & \Delta t \sum_{q=0}^{Q-1} h_1(q) s(t - q) \\
 & + (\Delta t)^3 \sum_{q_1=0}^{Q-1} \sum_{q_2=0}^{Q-1} \sum_{q_3=0}^{Q-1} h_3(q_1, q_2, q_3) s(t - q_1) s(t - q_2) s(t - q_3)
 \end{aligned} \tag{2}$$

where  $t$ ,  $q$ , and  $q_n$  are indices of sample points [6]. The time increment  $\Delta t$  is usually removed in normalization.  $Q$  is the number of samples over the *two-sided* bandwidth of the signal, giving  $Q$  time-domain samples in the kernel. Once  $h_1$  and  $h_3$  are known, the evaluation of this expression is straightforward, involving only multiplying and accumulating. The kernels  $h_1$  and  $h_3$  are determined from the modelled circuit’s frequency-domain responses, obtained from laboratory measurements or harmonic-balance simulations. The complex envelope equivalent is then generated and the kernel obtained by Fourier transformation. This requires a relatively large amount of data, which might require extensive harmonic-balance analyses or the use of a nonlinear network analyzer. The details of this process are the subject of the next section.

## Model Identification

The nonlinear transfer function  $H_n(\omega_1, \omega_2, \dots)$ , the frequency-domain equivalent of the kernel  $h_n(\tau_1, \tau_2, \dots)$ , is found from responses at discrete excitation frequencies within the modelled component's passband. The frequency components then are Fourier transformed to obtain a linear impulse-response function and a third-order Volterra kernel. For most kinds of components, a relatively small number of frequency samples is adequate; in a narrowband signal, we assume that 8 or at most 16 samples over the band of interest are enough. If a fast Fourier transform (FFT) is used, the number of samples must be a power of two. Later in this document, however, we show that an FFT may not be the best way, for practical reasons, to perform the frequency-to-time conversion. The system of interest is shown in Figure 1.

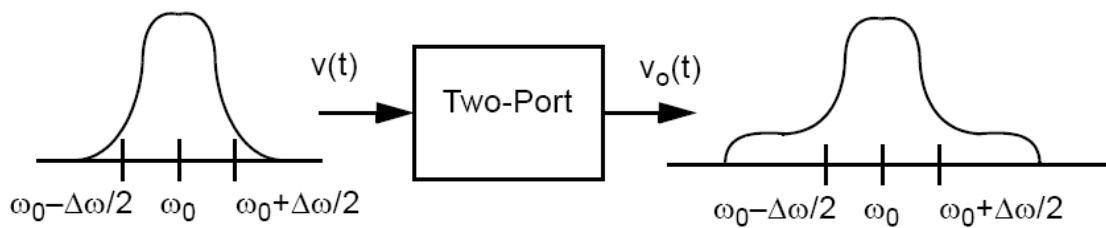


Figure 1: The system of interest is a narrow-band signal, such as a WCDMA waveform. This signal excites a two-port, typically a power amplifier resulting in a distorted waveform, which includes ACPR sidebands.

The excitation is a narrowband signal  $v(t)$  and the output of the nonlinear block is  $v_o(t)$ , which includes both the linear response and intermodulation sidebands. In the frequency domain, the first- and third-order components of  $v_o(t)$  are given by:

$$\begin{aligned}
 v_o(t) = & \frac{1}{2} \sum_{q=-Q}^Q V_q H(\omega_q) \exp(j\omega_q t) \\
 & + \frac{1}{8} \sum_{q_1=-Q}^Q \sum_{q_2=-Q}^Q \sum_{q_3=-Q}^Q V_{q_1} V_{q_2} V_{q_3} H_3(\omega_{q_1}, \omega_{q_2}, \omega_{q_3}) \exp(j(\omega_{q_1} + \omega_{q_2} + \omega_{q_3})t)
 \end{aligned} \tag{3}$$

where  $V_q$ ,  $V_{qn}$  are excitation-voltage components and  $H_3(\omega_{q1}, \omega_{q2}, \omega_{q3})$  is the third-order nonlinear transfer function. Only odd-order components are needed, as only these contribute to the first zone response. As we are dealing with narrowband signals, even-order components are invariably out-of-band. Initially we obtain first- (linear) and third-order components; these are adequate for calculating the first set of “shoulders” for ACPR analysis. Fifth-order responses could be included in an analogous manner, but the measurement or identification process would become much greater and more time-consuming.

Indeed, the process need not even be as complicated as (3) seems to imply. We can take advantage of several facts:

1. We need calculate only the positive-frequency components of the output signal, as we ultimately want only its complex-envelope representation;
2. A large number of the terms in the multiple summation in (3) are identical and need not be recalculated;
3. Not all the terms in the summation produce first-zone components, so many can be eliminated. Indeed, in the third-order triple summation, we need only two positive frequency input components and one negative-frequency. Then, (3) becomes:

$$\hat{v}_o(t) = \frac{1}{2} \sum_{q=1}^Q V_q H(\omega_q) \exp(j\omega_q t) + \frac{3}{8} \sum_{q_1=1}^Q \sum_{q_2=1}^Q \sum_{q_3=1}^Q V_{q_1} V_{q_2} V_{q_3}^* H_3(\omega_{q_1}, \omega_{q_2}, -\omega_{q_3}) \exp(j(\omega_{q_1} + \omega_{q_2} - \omega_{q_3})t) \quad (4)$$

where the circumflex indicates that includes only a subset of the frequency components in (3). Three-tone analyses are not necessary to obtain every third-order term in (3). Some third-order products (e.g.,  $2\omega_2 - \omega_1 = \omega_2 + \omega_2 - \omega_1$ ) are obtained by two-tone analysis of the modelled circuit, and other tones (e.g.,  $\omega_1 = \omega_1 + \omega_1 - \omega_1$ ), which occur at a fundamental frequency, can be obtained by a single-tone analysis.

To obtain the Volterra kernels, we probe the system with a number of discrete sinusoidal excitations,  $Q$ , uniformly spaced across the band, and calculate or measure the output components at both in-band and out-of-band frequencies. The model is extracted entirely from these input/output measurements. The situation is illustrated in Figure 2. Note that the excitations must be non commensurate, so the frequency points cannot be uniformly spaced. This is essential for proper model identification using three-tone excitations.

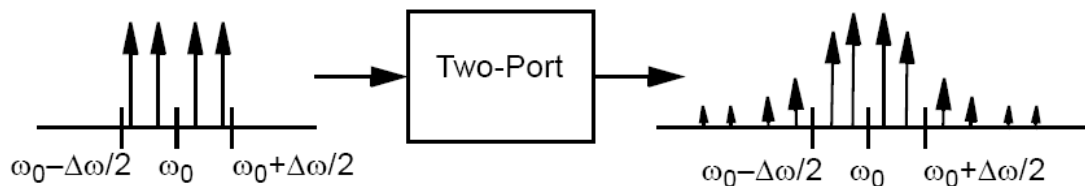


Figure 2: Volterra kernels are obtained by analysis at a number of discrete frequencies over the bandwidth of the signal.



### Linear Transfer Function

The linear transfer function,  $H_1(\omega)$ , is obtained in the usual manner:

$$H_1(\omega) = \frac{V_{o1}}{V_1} \quad (5)$$

where  $V_{o1}$  is the first-order (linear) component.  $H_1(\omega)$  must be evaluated over all frequency sample points in the component's passband. The transfer function is found either from a linear analysis of the circuit or from a nonlinear analysis with the signal level at least 10dB below the 1-dB compression point.  $V_1$  is the *source* voltage, not the *input* voltage, of the test circuit.

### Nonlinear Transfer Function Components Involving Single-Tone Products

The fundamental output is:

$$\begin{aligned} \hat{v}_{o3}(t) &= \frac{1}{8}(V_1 V_1 V_1^* H_3(\omega, \omega, -\omega) + V_1 V_1^* V_1 H_3(\omega, -\omega, \omega) + V_1^* V_1 V_1 H_3(-\omega, \omega, \omega)) \\ &= \frac{3}{8} V_1 V_1 V_1^* H_3(\omega, \omega, -\omega) \end{aligned} \quad (6)$$

where we have employed the principle of kernel symmetry. The frequency-domain (phasor) component  $V_{o3}$  is:

$$V_{o3} = \frac{3}{4} V_1 V_1 V_1^* H_3(\omega, \omega, -\omega) \quad (7)$$

so  $H_3$  is:

$$H_3(\omega, \omega, -\omega) = H_3(\omega, -\omega, \omega) = H_3(-\omega, \omega, \omega) = \frac{4}{3} \frac{V_{o3}}{V_1 V_1 V_1^*} \quad (8)$$

In (8),  $V_{o3}$  is the third-order component only; i.e., the fundamental component must be subtracted from the output voltage when the circuit is lightly saturated:

$$V_{o3} = V_o(\omega) - H_1(\omega) V_1 \quad (9)$$

which can be written:

$$H_3(-\omega, \omega, \omega) = \frac{4}{3} \left( \frac{V_o(\omega)}{V_1 V_1 V_1^*} - \frac{H_1(\omega)}{|V_1|^2} \right) \quad (10)$$



where  $V_o(\omega)$  is the total linear plus third-order output voltage at  $\omega$ .  $V_1$ , the source voltage, can always be made real in the circuit analysis, so the conjugate term in (8) is largely academic. Eq. (8) is evaluated at all sample frequencies over the component's passband.

*Nonlinear Transfer Function Components Involving Two-Tone Products*

These products have the form  $2\omega_1 - \omega_2$ , with  $\omega_1 \neq \omega_2$ . Then:

$$\begin{aligned} \hat{v}_{o3}(t) &= \frac{1}{8}(V_1 V_1 V_2^* H_3(\omega_1, \omega_1, -\omega_2) + V_1 V_2^* V_1 H_3(\omega_1, -\omega_2, \omega_1) \\ &\quad + V_2^* V_1 V_1 H_3(-\omega_2, \omega_1, \omega_1)) \\ &= \frac{3}{8} V_1 V_1 V_2^* H_3(\omega_1, \omega_1, -\omega_2) \end{aligned} \quad (11)$$

so the transfer function is:

$$H_3(\omega_1, \omega_1, -\omega_2) = \frac{4}{3} \frac{V_{o3}}{V_1 V_1 V_2^*} \quad (12)$$

The other transfer-function components at  $2\omega_2 - \omega_1$  follow similarly. The other components that must be determined by a two-tone analysis occur at the excitation frequencies. These are:

$$\omega_1 = \omega_1 + \omega_2 - \omega_2 \quad (13)$$

$$\omega_2 = \omega_2 + \omega_1 - \omega_1 \quad (14)$$

and, of course, their permutations. There are six such terms in the Volterra series for each of these, and it is necessary to remove the effects of the single-tone produces as well. Thus, for (13), we have:

$$\hat{v}_{o3}(t) = \frac{6}{8} V_1 V_2 V_2^* H_3(\omega_1, \omega_2, -\omega_2) + \frac{3}{8} V_1 V_1 V_1^* H_3(\omega_1, \omega_1, -\omega_1) + \frac{1}{2} V_1 H_1(\omega_1) \quad (15)$$

which is solved easily for  $H_3(\omega_1, \omega_2, -\omega_2)$ :

$$H_3(\omega_1, \omega_2, -\omega_2) = \frac{2}{3} \frac{V_{o3}}{V_1 V_2 V_2^*} - \frac{1}{2} \frac{|V_1|^2}{|V_2|^2} H_3(\omega_1, \omega_1, -\omega_1) - \frac{2}{3} H_1(\omega_1) \quad (16)$$

Note that all these terms can be found from a single harmonic-balance analysis.



### Nonlinear Transfer Function Components Involving Three-Tone Products

These have the form  $\omega_1 + \omega_2 - \omega_3$ . The output voltage is:

$$\begin{aligned} \hat{v}_{o3}(t) = & \frac{1}{8} [V_1 V_2 V_3^* H_3(\omega_1, \omega_2, -\omega_3) + V_2 V_1 V_3^* H_3(\omega_2, \omega_1, -\omega_3) \\ & + V_1 V_3^* V_2 H_3(\omega_1, -\omega_3, \omega_2) + V_2 V_3^* V_1 H_3(\omega_2, -\omega_3, \omega_1) \\ & + V_3^* V_1 V_2 H_3(-\omega_3, \omega_1, \omega_2) + V_3^* V_2 V_1 H_3(-\omega_3, \omega_2, \omega_1)] \end{aligned} \quad (17)$$

which gives, in a manner similar to the previous cases:

$$H_3(\omega_1, \omega_2, -\omega_3) = \frac{2}{3} \frac{V_{o3}}{V_1 V_2 V_3^*} \quad (18)$$

As with the two-tone products, the three-tone excitation generates components at the excitation frequencies. However, the nonlinear transfer functions that create them have the forms,  $H_3(\omega_1, \omega_2, -\omega_2)$  and similar, which are evaluated as part of the two-tone analyses. If the frequency spacings were uniform, it would also be possible to have a three-tone IM product coincident with an excitation frequency. That is, if the frequency spacing were  $\Delta\omega$ , we would have:

$$\omega_{IM} = \omega_1 - \omega_2 + \omega_3 = \omega_1 - (\omega_1 + \Delta\omega) + \omega_1 + 2\Delta\omega = \omega_2 \quad (19)$$

Avoiding this possibility is an important reason for using non uniform frequency intervals. If the frequency intervals were non uniform, the IM frequency might be close to  $\omega_2$ , but not coincident with it. In this case it is essential that the frequency intervals be sufficiently non uniform to avoid ill conditioning in the harmonic-balance analysis. As with the two-tone analysis, several transfer-function components can be found from a single three-tone analysis.

### Determination of the Kernels

We need to determine the time-domain kernels suitable for use with a complex-envelope signal for a restricted set of responses, namely, the first-zone response. Since conventional Volterra theory is based on real signals, it is necessary to derive this relation from first principles. Recall that (4) gave the *positive-frequency, first-zone* components in the vicinity of the carrier frequency,  $\omega_0$ . It is relatively easy to show that the form of (4) does not change appreciably in forming the complex envelope components; only a shift in frequency by  $\omega_0$  in all dimensions is necessary. This is analogous to the linear case, in which the complex envelope signal is given merely by frequency-shifting its positive-frequency spectrum. Specifically, the third order response in terms of the complex envelope,  $\tilde{v}_{o3}(t)$ , is:

$$\tilde{v}_{o3}(t) = \frac{3}{8} \sum_{q_1=1}^Q \sum_{q_2=1}^Q \sum_{q_3=1}^Q \tilde{V}_{q_1} \tilde{V}_{q_2} \tilde{V}_{q_3}^* \tilde{H}_3(\omega_{q_1}, \omega_{q_2}, -\omega_{q_3}) \exp(j(\omega_{q_1} + \omega_{q_2} - \omega_{q_3})t) \quad (20)$$

where the  $\omega_{qn}$  are now baseband frequency components, the tilde indicates complex-envelope quantities, and:

$$\tilde{H}_3(\omega_{q_1}, \omega_{q_2}, -\omega_{q_3}) = H_3(\omega_{q_1} + \omega_0, \omega_{q_2} + \omega_0, -(\omega_{q_3} + \omega_0)) \quad (21)$$



The excitation voltages are:

$$\tilde{V}_{qn} = \int_{-\infty}^{\infty} \tilde{v}_n(\tau) \exp(-j\omega_{qn}\tau) d\tau \quad (22)$$

where  $\tilde{v}_n(\tau)$  is the complex-envelope representation of the excitation signal. Substituting (22) into (20) and applying the change of variables:

$$t - \tau_n \rightarrow \alpha_n \quad (23)$$

gives, finally:

$$\begin{aligned} \tilde{v}_{o3}(t) = & \frac{3}{8} \int_{-\infty}^{\infty} \int_{-\infty}^{\infty} \int_{-\infty}^{\infty} \sum_{q_1=1}^Q \sum_{q_2=1}^Q \sum_{q_3=1}^Q \tilde{H}_3(\omega_{q_1}, \omega_{q_2}, -\omega_{q_3}) \exp(j(\omega_{q_1}\alpha_1 + \omega_{q_2}\alpha_2 - \omega_{q_3}\alpha_3)) \\ & \cdot \tilde{v}_1(t - \alpha_1) \tilde{v}_2(t - \alpha_2) \tilde{v}_3^*(t - \alpha_3) d\alpha_1 d\alpha_2 d\alpha_3 \end{aligned} \quad (24)$$

By inspection, the time-domain kernel is:

$$\tilde{h}_3(\alpha_1, \alpha_2, \alpha_3) = \frac{3}{8} \sum_{q_1=1}^Q \sum_{q_2=1}^Q \sum_{q_3=1}^Q \tilde{H}_3(\omega_{q_1}, \omega_{q_2}, -\omega_{q_3}) \exp(j(\omega_{q_1}\alpha_1 + \omega_{q_2}\alpha_2 - \omega_{q_3}\alpha_3)) \quad (25)$$

As expected, the time-domain kernel is a kind of truncated three-dimensional discrete Fourier transform of the frequency-domain data. This could be calculated by a fast Fourier transform (FFT); however, there are some good reasons not to do this:

1. The frequencies used in the harmonic-balance analysis would have to correspond to the time-sample rate and sequence length used in the system analysis. For various reasons, the user might want to use a different rate or sequence length.
2. The frequencies must also be non commensurate, so the frequency steps across the band must be non uniform. Otherwise, the extraction of the transfer function becomes quite a bit more difficult, perhaps impossible. This probably would not work with an FFT.
3. It is desirable for the user to be able to change the time sampling without having to perform a new harmonic-balance analysis. To do this, some kind of interpolation would be necessary. With a three-dimensional FFT, it would be necessary first to perform a three-dimensional interpolation in the frequency domain, or, perhaps, to perform the interpolation in the time domain after generating the time-domain kernel. This is likely to be a computationally costly process, and could introduce artefacts.
4. In some cases it may be desirable to have non uniform sampling in the frequency domain. This is particularly the case when long-term memory in power amplifiers must be simulated. Users might also want a number of sample points that is not restricted, as in FFTs, to a power of 2.



Another approach is to calculate  $h_3(\alpha_1, \alpha_2, \alpha_3)$  in a “brute force” manner; that is, through the multiple summations indicated in (25). This is computationally more costly than an FFT, but the computation time is undoubtedly small compared to the harmonic-balance analyses. As a major advantage, however, it provides a straightforward method for interpolation. The errors introduced by Fourier interpolation are well known (e.g., Gibbs effect) and should not be a serious problem in the smoothly varying transfer functions we expect. If the transfer function includes significant poles close to the passband, as might occur in circuits that have significant filtering, artefacts may appear. These probably can be avoided by decreasing the frequency domain sampling interval, or, better, placing the filters in the system model instead of the circuit. The only remaining important restriction is that some  $\omega_{qn}$  must equal  $\omega_0$ . This is not a terribly restrictive requirement.

To ease the evaluation, one can write (25) as:

$$\tilde{h}_3(\alpha_1, \alpha_2, \alpha_3) = \frac{3}{8} \sum_{q_1=1}^Q \sum_{q_2=q_1}^Q \sum_{q_3=1}^Q (2 - \delta_q) \tilde{H}_3(\omega_{q_1}, \omega_{q_2}, -\omega_{q_3}) \cdot \exp(j(\omega_{q_1}\alpha_1 + \omega_{q_2}\alpha_2 - \omega_{q_3}\alpha_3)) \quad (26)$$

Where:

$$\delta_q = \begin{cases} 1 & q_1 = q_2 \\ 0 & q_1 \neq q_2 \end{cases} \quad (27)$$

Then, since  $h_3(\alpha_1, \alpha_2, \alpha_3) = h_3(\alpha_2, \alpha_1, \alpha_3)$  one need only evaluate  $\alpha_2 \geq \alpha_1$  and fill in the values for  $\alpha_2 < \alpha_1$ .

It is interesting to note that the expression (25) is much simpler than those in the classical treatise by Benedetto et al. [8]. In the latter, the time-domain complex-envelope kernel is derived directly from a kernel representing real signals. In the above derivation, the conversion from real to complex-envelope form is performed in the frequency domain, so the complex-envelope calculation has the same form as for a real signal. This should make calculations using this model in VSS simpler and faster.

## Calculation Process in VSS

### Sampling Rates

In VSS, the sampling rate, `_DRATE`, must be set to at least  $2B$ , where  $B$  is the *two-sided* bandwidth of the undistorted input signal. This is double the Nyquist rate based on the input bandwidth, but is necessary to resolve the third-order output IM products, which extend over twice the input bandwidth. Similarly, if the input band is divided into  $Q$  frequency points for the harmonic-balance analysis, the oversampling rate, `_SMPSYM`, ideally should be  $2Q$ . In practice, the frequency resolution of the analysis may differ from that used in the harmonic balance analysis. If this resolution is  $\Delta f$ , the time window for each dimension of  $h_3(\alpha_1, \alpha_2, \alpha_3)$  must be  $1/\Delta f$ . The maximum time interval between samples is  $1/2B$ , so at least  $(1/\Delta f)/(1/2B) = 2B/\Delta f$  time samples, in each dimension, are needed. Another criterion affecting sampling rates is the need to resolve long-term memory effects. If the characteristic time for memory effects (e.g., a thermal time constant) is  $T$ , each dimension of  $h_3(\alpha_1, \alpha_2, \alpha_3)$  must be at least this long. Thus, the window is  $T$  and the minimum number of samples is  $2BT$ . In this case, however, the harmonic-balance



analyses must include adequate low-frequency components, so that the long-term effects are included in the time-domain kernel. This requires, in turn, analysis at sideband frequencies on the order of  $1/T$ . It should be noted that the complete modelling of memory effects is probably more complex than a first-order/third-order analysis. It is possible that certain effects, especially bias-circuit phenomena, require a second-order component to the analysis, and perhaps even greater orders than third may be necessary as well. Lacking a general theory of such phenomena, it is difficult to determine, with any precision, what is needed in such a model.

#### *Calculation of the Output Waveform*

The output consists of one- and three-dimensional convolutions given by (2). Evaluating these is simply a matter of going through the indicated summations. There is probably no simpler way to do it.

#### **References**

- [1] J. Vuolevi, T. Rahkonen, *Distortion in RF Power Amplifiers*, Artech House, Norwood, MA, 2003.
- [2] M. Schetzen, "Nonlinear System Modelling Based on the Wiener Theory", *Proc. IEEE*, vol. 69, No.12, p.1557, Dec. 1981.
- [3] M. Schetzen, *The Volterra and Wiener Theories of Nonlinear Systems*, John Wiley & Sons, New York, 1980.
- [4] J. C. Pedro and S. A. Maas, "A Comparative Overview of Microwave and Wireless Power-Amplifier Behavioural Modelling Approaches," *IEEE Trans. Microwave Theory Tech.*, vol. 53, p. 1150, 2005.
- [5] J. C. Pedro, "Modelling and Simulation of Nonlinear RF Systems" AWR Report, August, 2003.
- [6] S. A. Maas, "Volterra Analysis of Spectral Regrowth," *IEEE Trans. Microwave Theory Tech.*, vol. 7, p. 192, 1997.
- [7] S. A. Maas, *Nonlinear Microwave and RF Circuits*, Artech House, Norwood, MA, 2003.
- [8] S. Benedetto, E. Biglieri, and R. Daffara, "Modelling and Performance of Nonlinear Satellite links—A Volterra Approach," *IEEE Trans. Aerospace and Elect. Sys.*, vol. AES-15, p. 494, 1979.